Acta Pharmacologica Sinica

www.nature.com/aps

ARTICLE

G protein-coupled receptor kinase 2 as a novel therapeutic target for gland fibrosis of Sjögren's syndrome

Ru-hong Fang[1], Zheng-wei Zhou[1,2], Rui Chu[1], Qiu-yun Guan[1], Feng He[1], Ming-li Ge[1], Pai-pai Guo[1], Hua-xun Wu[1], Ling-li Yao[3], Wei Wei[1]✉, Yang Ma[1]✉ and Qing-tong Wang[1,4]✉

Sjogren's syndrome (SS) is a chronic, progressive autoimmune disorder characterized by gland fibrosis. We previously found a close correlation between gland fibrosis and the expression of G protein-coupled receptor kinase 2 (GRK2). In this study we explored the pathological and therapeutic significance of GRK2 in SS. Submandibular gland (SMG) antigen-induced SS mouse model was established in WT and GRK2$^{+/-}$ mice. We showed that the expression levels of GRK2 were significantly up-regulated in glandular tissue and positively correlated with fibrotic morphology in SS patients and mice. Hemizygous knockout of GRK2 significantly inhibited the gland fibrosis. In mouse salivary gland epithelial cells (SGECs), we demonstrated that GRK2 interacted with Smad2/3 to positively regulate the activation of TGF-β-Smad signaling with a TGF-β-GRK2 positive feedback loop contributing to gland fibrosis. Hemizygous knockout of GRK2 attenuated TGF-β-induced collagen I production in SGECs in vitro and hindered gland fibrosis in murine SS though preventing Smad2/3 nuclear translocation. Around 28 days post immunization with SMG antigen, WT SS mice were treated with a specific GRK2 inhibitor paroxetine (Par, 5 mg·kg^{-1}·d^{-1}, i.g. for 19 days). We found that Par administration significantly attenuated gland fibrosis and alleviated the progression of SS in mice. We conclude that genetic knockdown or pharmacological inhibition of GRK2 significantly attenuates gland fibrosis and alleviates the progression of SS. GRK2 binds to Smad2/3 and positively regulates the activation of TGF-β-Smad signaling. A TGF-β-GRK2 positive feedback loop contributes to gland fibrosis. Our research points out that GRK2 could be a promising therapeutic target for treating SS.

Keywords: Sjögren's syndrome; SGECs; GRK2; Smad2/3; gland fibrosis; paroxetine

Acta Pharmacologica Sinica (2024) 0:1–14; https://doi.org/10.1038/s41401-024-01350-4

INTRODUCTION

Sjögren's syndrome (SS) is an autoimmune disease which occurs in 0.5%–1.0% of the population worldwide [1]. SS is characterized by chronic exocrine gland inflammation with infiltration of lymphocytes and occurs more commonly in women, with a male-to-female ratio of 1:9 to 1:20 [1]. Its main clinical features include dental diseases, parotid gland enlargement, dry mouth, and dry eyes [2, 3]. Although most studies denote that it is linked to environmental, genetic, and endocrine factors, the etiology of SS is still unclear [4]. The inflammation evoked by T and B lymphocytes has been considered to be the crucial initiator for the development and occurrence of SS [5]. Importantly, salivary gland epithelial cells (SGECs) play a key role in the pathogenesis of SS, also known as autoimmune epithelitis [6, 7]. Chronic exposure to pro-inflammatory mediators may drive submandibular gland (SMG) fibrosis via an epithelial-mesenchymal transition (EMT)-dependent fibrotic process [8–10]. In the context of SS, the submandibular gland (SMG) fibrosis emerges as a pivotal outcome of compromised secretory function, playing a crucial role in the architectural reconfiguration of the glandular tissue as the disease evolves [11, 12]. Despite its significance, comprehensive investigation into this phenomenon remains lacking. Considering the gradual and subtle progression of SS, clinical observations frequently reveal a prevalent co-occurrence of glandular dysfunction and fibrosis among patients [13]. This highlights the necessity for a concentrated research effort to better understand and address SMG fibrosis within the SS pathology.

Currently, there is no ideal treatment for SS clinically. Symptomatic and immunosuppressive therapies, such as salivary stimulants, methotrexate, and glucocorticoids, are commonly used to relieve the symptoms and delay the disease progression. However, these treatments have serious adverse reactions, such as hypertension and peptic ulcers, and only provide temporary relief [14]. Although biological agents are effective for gland-related manifestations, the therapeutic range is narrow [15]. Hydroxychloroquine (HCQ) is the first-line treatment for inflammatory musculoskeletal pain related to SS, according to the latest clinical practice guidelines by the SS Foundation [16]. While some studies have revealed that HCQ can improve gland-related manifestations, its long-term benefit on SS patients still need to be evaluated [17].

[1]Institute of Clinical Pharmacology, Anhui Medical University, Key Laboratory of Anti-inflammatory and Immune Medicine, Ministry of Education, Collaborative Innovation Center of Anti-Inflammatory and Immune Medicine, Hefei 230032, China; [2]Department of Pharmacy, Lu'an Hospital of Anhui Medical University, Lu'an People's Hospital of Anhui Province, Lu'an 237006, China; [3]Department of Pathology, the First Affiliated Hospital of University of Science and Technology of China (Anhui Provincial Hospital), Hefei 230001, China and [4]The Third Affiliated Hospital of Anhui Medical University (the First People's Hospital of Hefei), Hefei 230061, China
Correspondence: Wei Wei (wwei@ahmu.edu.cn) or Yang Ma (mayang@ahmu.edu.cn) or Qing-tong Wang (qingtongwang@ahmu.edu.cn)
These authors contributed equally: Ru-hong Fang, Zheng-wei Zhou

Received: 26 January 2024 Accepted: 2 July 2024
Published online: 25 July 2024

Therefore, there is an urgent need for safe and effective drugs with fewer side effects to treat SS.

G protein-coupled receptor kinase-2 (GRK2), one of the important serine (Ser)/threonine (Thr) kinases, is known to phosphorylate a number of G protein-coupled receptors (GPCRs) and non-GPCR substrates [18–20]. Besides the classical role in regulating GRCR responses, GRK2 is a versatile scaffold protein that interacts with multiple signaling molecules under different pathophysiological conditions. Especially, several experiments suggested that the increased GRK2 in CFs induces the deposition of extracellular matrix (ECM) and some evidence suggests that abnormal expression or activity of GRK2 participates in the regulation of fibrosis-associated pathways, thus GRK2 plays an essential role in the development of fibrotic diseases [21]. Inhibition or depletion of GRK2 has been shown to reduce the expression of fibrotic genes and attenuate fibrosis in various organs and tissues, including the lungs [22], heart [23], and kidneys [24]. However, its modulation mechanisms on fibrosis and functions involved in gland fibrosis during the process of SS has not been well addressed.

As the key regulator of tissue fibrosis, transforming growth factor-β (TGF-β) promotes fibrosis by activating fibroblasts to obtain myofibroblast phenotype, having epithelial cells undergo EMT, and eventually increasing ECM synthesis [25, 26]. TGF-β binds to type I/II TGF-β receptor tetramer which phosphorylates the receptor-activated Smads (R-Smads), Smad2 and 3. When phosphorylated, the R-Smad complexes with Smad4, allowing it to translocate into the nucleus where it regulates the expression of various fibrotic genes [27, 28]. Moreover, TGF-β can cause non-canonical pathway activation through mechanisms including extracellular regulated protein kinase (ERK), JUN N-terminal kinases (JNK), mitogen-activated protein kinase (MAPK), and phosphoinositide 3-kinase (PI3K) pathways, which are known to crosstalk with Smad pathways at multiple levels [11, 29, 30]. Previous studies have reported that the expression of GRK2 can be induced by TGF-β both in lung fibroblast cells and cardiac fibroblasts [22, 23], suggesting there is a possible alternative pathway of TGF-β-GRK2 activity in the pathogenesis of EMT. However, the effect of GRK2 on Smad2/3 activation in EMT of SGECs has not been revealed.

In the current study, the SMG antigen-induced SS mouse model was established in GRK2$^{+/-}$ and WT mice, and the manifestations were compared by monitoring water intake, saliva volume, and pathological changes in glands. The fibrosis of glands was evaluated though Masson's staining and collagen I detection. As detected, hemizygous knockout of GRK2 attenuated TGF-β-induced collagen I production in SGECs and hindered gland fibrosis in murine SS. Mechanically, GRK2 interacted with Smad2/3 to positively regulate the activation of Smad2/3 induced by TGF-β1 in SGECs. Inhibiting GRK2 by an established GRK2 inhibitor Paroxetine (Par) significantly attenuated gland fibrosis and alleviated the progression of SS in mice, indicating that GRK2 is a therapeutic target to treat gland fibrosis in SS.

MATERIALS AND METHODS

Patient specimens

The experimental protocols were approved by Research Ethics Committees of Anhui Medical University. Labial gland biopsies were obtained from patients referred for suspected pSS underwent labial gland biopsies due to the absence of detectable anti-Ro/SSA antibodies in their blood tests at the Rheumatology Department of the First Affiliated Hospital of the University of Science and Technology of China (Anhui Provincial Hospital). pSS was defined according to the 2016 American College of Rheumatology/European League Against Rheumatism criteria (Supplementary Table S1), and controls were patients presenting sicca symptoms without anti-Ro/SSA antibodies and with normal or subnormal labial gland (ie, focus score of <1).

Briefly, cotton balls were inserted into both sides of the lower lip and buccal mucosa of patients to minimize excessive saliva secretion and contamination. The skin and mucosa on the surface of the labial gland, upper and lower lips were disinfected prior to placing a sterile towel. The mucosal epithelium was removed by performing a fusiform incision at the surgical site, and the labial gland tissues were carefully collected. The excised tissues were fixed in formalin solution for the subsequent examinations. Labial gland tissue paraffin blocks of diagnosed SS patients and control patients were then sliced in the Department of Pathology. The relevant experiments were conducted with informed consent. All participants provided written informed consent.

Animals

Female WT mice aged 6–8 weeks (Certificate No. SCXK(WAN), 2011-002) were procured from the Animal Department of Anhui Medical University (Hefei, China), while female GRK2$^{+/-}$ mice aged 6–8 weeks were ordered from GemPharmatech Co., Ltd (Nanjing, China). All animals were housed in a specific pathogen-free facility and all experimental procedures were approved by the Ethical Review Committee for Animal Experimentation at the Institution of Clinical Pharmacology, Anhui Medical University. Animal studies were conducted in compliance with the ARRIVE guidelines.

Mouse SGECs isolation

WT and GRK2$^{+/-}$ mice were sterilized with 75% alcohol, and SMG tissues were collected by removing the adipose and connective tissues. The dissected tissues were then washed, finely shredded, and subjected to pancreatic enzyme (Cat # C3538-0100, Shanghai XP Biomed Co., Ltd, Shanghai, China) digestion. The suspension was shaken and filtered. Finally, the filtered suspension was centrifuged, resuspended with cell culture media, and seeded on gelatin-coated petri dishes.

Induction of SS and treatment

Bilateral SMGs were extracted from WT mice and the protein concentration was quantified after homogenization. The SMG protein was emulsified in an equal volume of Freund's complete adjuvant (Cat # F5881, Sigma, MO, USA) containing 4 mg/mL Bacillus Calmette-Guerin to a final concentration of 2 mg/mL. At day 0 and 7, the immunized group of WT and GRK2$^{+/-}$ mice received a subcutaneous injection of 0.15 mL emulsion per mouse on the back and tail. On day 14 after the first immunization, SMG proteins (2 mg/mL) emulsified in Freund's incomplete adjuvant (Cat # F5506, Sigma, MO, USA) were subcutaneously injected. Control mice were injected with saline. Around 28 days post immunization, mice developed SS symptoms and WT SS mice were randomly divided and gavaged with: Par (5 mg/kg, SK&F Pharm, Co., Ltd, Tianjin, China; SS-Par), HCQ (80 mg/kg, Shanghai Zhongxi Pharmaceutical (Group) Co., Ltd, Shanghai, China; SS-HCQ), or vehicle (0.25% sodium carboxymethyl cellulose, CMC-Na; SS-Veh). The body weight of the mice was measured weekly, along with their water intake.

Salivary flow rate and SMG index

Saliva volume was assessed weekly by injecting 0.125 mg/mL Pilocarpine Hydrochloride (Cat # HY-B0726, MedChemexpress Co., Ltd, Shanghai, China) into the abdominal cavity of anesthetized mice, and secreted saliva was collected within 10 min using sterile cotton balls placed under their tongues. The weight difference of cotton balls before and after collection represented the amount of saliva. After euthanizing the animals, the salivary gland was excised and weighed to determine the SMG index, which was calculated as a percentage of the SMG weight (g) relative to mouse weight (g).

Imaging and bloodstream signal detection and evaluation
Before the mice were sacrificed, the structure and blood flow signals of SMGs were determined on a small animal ultrasound imaging system (Vevo2100, FUJIFILM VisualSonics, Toronto, ON, Canada). The blood flow signals were semi-quantified as: 0 points, there is 0 to 1 blood flow spots inside the glands; 1 point, there are only 2 to 3 small blood spots inside the gland; 2 points, there are 4 to 5 blood flow spots in the gland; 3 points, there are 6 or more blood flow spots in the gland.

ELISA assay
When mice were anesthetized and sacrificed, peripheral blood was collected and incubated at 4 °C to clot before centrifugation at 3000 × *g* for 15 min. The supernatant was then collected to detect the expression of TGF-β1, IgG and β-2 microglobulin according to TGF-β1 ELISA kit (Cat # EK981-96, MultiSciences (Lianke) Biotech co., Ltd, Zhejiang, China), IgG (Cat # ELK5100, ELK Biotechnology Co., Ltd, Wuhan, China), or β-2 microglobulin ELISA kit (Cat # ELK1391, ELK Biotechnology Co., Ltd, Wuhan, China) instructions.

Histopathological assessment and Masson's staining
Mice SMGs and human lip gland tissue blocks were sliced and subjected to hematoxylin and eosin (H&E) staining as well as Masson's staining using the method described previously [24]. Histopathological changes were evaluated according to Chisholm and Masson's method: grade 0: the acinar and ducts are normal, and there is no lymphocyte infiltration; grade 1: mildly scattered in lymphocyte infiltration and plasma cells; grade 2: occasional atrophy of acinar and moderately scattered lymphocyte infiltration, but <50 cells/4 mm^2; grade 3: partial acinar atrophy and intralobular catheter dilation, 1 foci of interstitial lymphocyte infiltration and mild interstitial collagenization; grade 4: more than 1/3 acinar atrophy destruction and interlobar catheter dilation, and more than 2 foci of interstitial lymphocyte infiltration, and severe interstitial collagenization (Supplementary Table S2, S3) [25]. ImageJ software (NIH, Bethesda, MD, Version 1.42q) was applied to analyze the blue staining area of Masson's staining to indicate the level of fibrosis.

Immunofluorescence staining
Frozen sections were rehydrated with 0.5% Triton X-100 (Cat # P0096, Beyotime Biotechnology, Shanghai, China), and immersed in antigen retrieval solution containing EDTA (Cat # P0084, Beyotime Biotechnology, Shanghai, China). Non-specific binding was blocked by incubating with 5% bovine serum albumin (Cat # BS114, biosharp life sciences, Shanghai, China) for 2 h. The slides were then incubated with primary antibody overnight at 4 °C. The primary antibodies were as follows: mouse-anti Vimentin (Cat # 60330-1-Ig, Proteintech Group, Inc., Chicago, USA, 1:200 dilution), rabbit monoclonal Smad2/3 antibody (Cat # AF6367, Affinity Bioscience, OH, USA, 1:200 dilution), rabbit-anti β-catenin (Cat # 51067-2-AP, Proteintech Group, Inc., Chicago, USA, 1:200 dilution), rabbit-anti NF-κB (Cat # 10745-1-AP, Proteintech Group, Inc., Chicago, USA, 1:200 dilution), rabbit-anti ERK (Cat # 11257-1-AP, Proteintech Group, Inc., Chicago, USA, 1:200 dilution), or mouse-anti GRK2 (Cat # sc-13143, Santa Cruz Biotechnology, Dallas, TX, USA, 1:100 dilution). And the tissue sections subsequently were stained with fluorescent-coupled secondary antibody including Alexa Fluor 488-anti-mouse (Cat # 615-545-214, Jackson ImmunoResearch Inc., PA, USA, 1:200 dilution) or Alexa Fluor 647-anti-rabbit (Cat # 111-605-045, Jackson ImmunoResearch Inc., PA, USA, 1:200 dilution) for 1 h at room temperature in the dark followed by 3 TBST rinses. Nuclei were stained with DAPI (Cat # BL105A, biosharp life sciences, Shanghai, China), and images were captured using a confocal microscope (SP8, Leica, Wetzlar, Germany). Colocalization rate was analyzed using the Leica LAS-AF software (version 4.0.0, Mannheim, Germany) and mean fluorescence intensity (MFI) of each protein was semi-quantified by ImageJ software (NIH, Bethesda, MD, version 1.42q).

Meanwhile, SGECs of WT mice were seeded on coverslips in 24-well plates, which were categorized into five groups: control group (0.1% DMSO, Cat # ST038, Beyotime Biotechnology, Shanghai, China), TGF-β1 (10 ng/mL, Cat # P00199, Solarbio Science & Technology Co., Ltd, Beijing, China) group, SS mouse serum (20 ng/mL) group, TGF-β1 (10 ng/mL, Cat # P00199, Solarbio Science & Technology Co., Ltd, Beijing, China) and A8301 (10 μM, Cat # HY-10432, MedChemExpress Co., Ltd, Monmouth Junction, NJ, USA) group, SS serum (20 ng/mL) and A8301 (10 μM, Cat # HY-10432, MedChemExpress Co., Ltd, Monmouth Junction, NJ, USA) group, while SGECs of $GRK2^{+/-}$ mice were divided into control group (0.1% DMSO, Cat # ST038, Beyotime Biotechnology, Shanghai, China) and TGF-β1 (10 ng/mL, Cat # P00199, Solarbio Science & Technology Co., Ltd, Beijing, China) group, respectively. Then SGECs were fixed with 4% paraformaldehyde (Cat # P0099, Beyotime Biotechnology, Shanghai, China), and permeabilized with 0.3% Triton X-100 (Cat # P0096, Beyotime Biotechnology, Shanghai, China). After blocking with 5% goat serum (Cat # C0265, Beyotime Biotechnology, Shanghai, China), the cells were incubated with the primary antibody including anti-mouse Vimentin antibody (Cat # 60330-1-Ig, Proteintech Group, Inc., Chicago, USA, 1:200 dilution), anti-rabbit Smad2/3 antibody (Cat # AF6367, Affinity Bioscience, OH, USA, 1:200 dilution), or anti-mouse GRK2 antibody (Cat # sc-13143, Santa Cruz Biotechnology, Dallas, TX, USA, 1:100 dilution) at 4 °C overnight and then was treated as the follow-up of a frozen section.

Immunohistochemistry
Formalin-fixed, paraffin-embedded tissue sections were initially deparaffinized with xylene, rehydrated, and then subjected to antigen retrieval in 0.01 M citrate buffer (pH = 6.0) for 3 min at 95 °C. The sections were then incubated with primary antibody including anti-mouse Vimentin antibody (Cat # 60330-1-Ig, Proteintech Group, Inc., Chicago, USA, 1:100 dilution) or anti-rabbit TGF-βRI (Cat # sc-101574, Santa Cruz Biotechnology, Dallas, TX, USA, 1:100 dilution) overnight at 4 °C, followed by an incubation with the corresponding horseradish peroxidase-linked secondary antibody (Cat # PV-9000, ZSGB-BIO, Beijing, China) for 2 h at room temperature. Finally, the sections were counterstained with DAB (Cat # ZLI-9018, ZSGB-BIO, Beijing, China), sealed with mounting solution, and observed under an upright microscope (BX53, Olympus, Tokyo, Japan), and the percentage of positively stained cells was calculated.

Western blot
Proteins extracted from mouse SMG tissues and mouse SGECs were separated by SDS-PAGE, and transferred onto PVDF membranes (Millipore Corporation, Billerica, MA, USA). Subsequently, the membranes were blocked in 5% nonfat milk dissolved in TBST for 2 h, and incubated with the indicated primary antibodies including anti-mouse GRK2 (Cat # sc-13143, Santa Cruz Biotechnology, Dallas, TX, USA, 1:500 dilution), anti-rabbit Smad2/3 (Cat # AF6367, Affinity Bioscience, OH, USA, 1:1000 dilution), anti-rabbit phosphor-Smad2/3 (Cat # AF3367, Affinity Bioscience, OH, USA, 1:500 dilution), anti-rabbit collagen I (Cat # AF7001, Affinity Bioscience, OH, USA, 1:1000 dilution), or GAPDH (Cat # AF0911, Affinity Biosciences, OH, USA, 1:5000) diluted in primary antibody dilution buffer (Cat # P0023A, Beyotime Biotechnology, Shanghai, China), and then incubated with corresponding horseradish peroxidase conjugated goat anti-mouse IgG (H + L) secondary antibody (Cat # S0002, Affinity Biosciences, OH, USA, 1:20,000 dilution) or goat anti-rabbit IgG (H + L) secondary antibody (Cat # S0001, Affinity Biosciences, OH, USA, 1:20,000 dilution) for 2 h at 37 °C. Enhanced Chemiluminescence Western blotting substrate (Cat # 32106, Thermo Fisher Scientific, Waltham, MA, USA) was applied for band detection on an ImageQuant LAS 500 Imager (GE Healthcare Systems, Chicago, IL, USA). Five replicates were performed, and the results depicted reproducibility.

Co-immunoprecipitation (Co-IP)

A Co-IP experiment was performed to determine whether GRK2 interacts with Smad2/3 protein. Mouse SMG tissues from control, SS-Veh, and SS-Par were lysed with NP40 IP buffer. After centrifugation at 12,000 × *g* for 15 min at 4 °C, the supernatants of tissue lysates were collected and protein concentrations were determined by BCA Protein Assay kit (Cat # 23225, Thermo Fisher Scientific Inc., MA, USA). 1 mg protein was preincubated with 10 µL Protein A/G plus-agar beads (Cat # sc-2003, Santa Cruz Biotechnology, Dallas, TX, USA) and 2 µg mouse IgG control antibody (Cat # sc-2025, Santa Cruz Biotechnology, Dallas, TX, USA) for 2 h at 4 °C. They were then collected by spinning at 3000 × *g* for 5 min at 4 °C. A portion of the supernatant was retained for input assays. The precleared protein then was rotated with 10 µL of Protein A/G PLUS-Agarose beads which were incubated with anti-GRK2 antibody (Cat # sc-13143, Santa Cruz Biotechnology, Dallas, TX, USA) overnight at 4 °C. The next day, the protein supernatant and Protein A-Agarose were centrifuged at 3000 × *g* at 4 °C and washed three times with PBS containing protease inhibitors, followed by Western blot with the primary antibodies anti-mouse GRK2 (Cat # sc-13143, Santa Cruz Biotechnology, Dallas, TX, USA, 1:500 dilution), anti-rabbit Smad2/3 (Cat # AF6367, Affinity Bioscience, OH, USA 1:1000 dilution), or GAPDH (Cat # AF0911, Affinity Biosciences, OH, USA, 1:5000).

Statistical analysis

All data analysis occurred in GraphPad Prism 7 and values were expressed as mean ± SEM. Differences between three or more groups were evaluated by either one-way ANOVA with Tukey's posttest or two-way ANOVA with Sidak's posttest, as indicated. A *t* test was used to compare the differences between two groups. *P* values less than 0.05 were considered significant.

RESULTS

GRK2 knockdown hindered the gland fibrosis of antigen-induced SS

SS is a slowly progressive systemic autoimmune disease characterized by inflammation and lymphocytic infiltration in the salivary and labial glands with loss of function and dryness of mouth and eyes [2, 3]. H&E staining of the labial gland tissues of SS patients and SMG tissues of SS mice demonstrated lymphocyte infiltration in the glandular interstitium, dilation of ducts, and glandular disorganization. Of note, the structure of SS glands was distinctly remodeled. Further Masson's staining determined that severe collagen deposition and gland fibrosis presented in patients and mice with SS compared with healthy controls (Fig. 1a, b, Supplementary Fig. S1a, b). Until recently, accumulating studies were focused on the inflammation-mediated SS progression [12, 15, 17], but the mechanisms of gland fibrosis in SS pathogenesis were poorly studied. We have previously revealed that Par (Supplementary Table S4) could effectively improve a mouse model of SS [5, 31]. Here it can be further seen that in the SMG antigen-induced SS mouse model, Par treatment successfully reduced collagen deposition and the fibrotic marker Vimentin expression in salivary glands while also relieving the infiltration of lymphocytes (Fig. 1c, Supplementary Fig. S1c), suggesting Par effectively ameliorates gland fibrosis and hinders the progression of SS in mice, indicating that GRK2 may mediate the gland fibrosis in SS. In addition, GRK2 expression was significantly increased in the labial gland tissue of SS patients (Fig. 1d) when compared with healthy controls. To further confirm the characteristics of GRK2 expression in damaged salivary glands, an SS mouse model was established, and it revealed that GRK2 was significantly increased in mouse SMG tissues upon symptom progression (Fig. 1e). GRK2 expression is significantly correlated with fibrotic area, suggesting that GRK2 expression is increased in the salivary gland tissues in SS and might be tightly associated with gland fibrosis (Fig. 1f). To investigate the direct role of GRK2 in gland fibrosis in SS mice, the $GRK2^{+/-}$ (homozygous knockout is fatal) and littermate WT mice were subjected to SS development by SMG antigen challenge. H&E staining identified that the SMG tissues of WT SS mice were severely infiltrated with lymphocytes and underwent atrophy of the glandular follicles, while these pathological changes were substantially prevented in that of $GRK2^{+/-}$ SS mice (Fig. 1g, Supplementary Fig. S1d). Most importantly, collagen deposition in salivary glands was increased in WT SS mice and decreased dramatically in $GRK2^{+/-}$ SS mice (Fig. 1g, Supplementary Fig. S1e), suggesting that hemizygous knockout of GRK2 significantly inhibited gland fibrosis. These results indicated that GRK2 hemizygous knockout hindered antigen-induced SS gland fibrosis. However, the underlying mechanisms of GRK2 in promoting gland fibrosis of SS is unclear.

TGF-β-Smad signaling was highly activated in SGECs of SMG in SS mice

To investigate which signaling pathway is activated in the process of gland fibrosis, the immunofluorescence of fibrosis-related pathways in the Vimentin positive cells of mouse SMG tissues, including β-catenin, Smad2/3, NF-κB and ERK were detected. Vimentin was abundantly expressed in the gland tissue of SS mice. It was further found that all of these four transcriptional factors were upregulated both in the cytosol of gland cells and the nuclei of SGECs at various degrees. However, the nuclear distribution of Smad2/3 was dramatically elevated in SS mice compared with normal mice (Fig. 2a, b). Correspondingly, the protein phosphorylation of Smad2/3 was also increased in SMG tissues of SS mice (Supplementary Fig. S2a), indicating Smad2/3 signaling pathway is distinctly activated in the process of gland fibrosis. Consistent with prior research indicating IgG [32] and β2-microglobulin [33] could be reliable markers for disease activity in SS. we quantified the levels of these biomarkers in the serum of SS mice. The results demonstrated significantly elevated levels of IgG and β-2 microglobulin in SS mice (Fig. 2c). As a key cytokine for pro-fibrosis, TGF-β1 mediates the activation and nucleus translocation of Smad2/3 signaling to play a pivotal pro-fibrotic role in a variety of tissues [19]. Thus, TGF-β1 expression in serum and its receptor TGF-βRI expression in SMG tissues of mice were detected. Secretion of TGF-β1 was elevated in SS mice, and much more TGF-βRI was expressed in the labial gland tissue of SS patients as well as in SMGs of mice (Fig. 2d–f). Immunohistochemistry results also revealed that TGF-βRI was mostly distributed in SGECs and connective tissues and a small amount was expressed in interfollicular proliferating fibroblasts (Fig. 2e, f). The function of TGF-β1 signaling in activating SGECs was then verified. As expected, TGF-β1 or SS mouse serum markedly evoked collagen I synthesis and the phosphorylation of Smad2/3; while pretreatment with TGF-βRI inhibitor A8301 significantly prevented TGF-β-1 or SS serum-induced collagen I expression and Smad2/3 activation (Fig. 2g). Meanwhile, nuclear translocation of Smad2/3 was promoted by either TGF-β1 or SS mouse serum and was inhibited by inhibiting TGF-βRI in mouse SGECs (Supplementary Fig. S2b, c). These data confirm that TGF-β1-TGF-βRI-Smad2/3 signaling contributes to the activation of SGECs and collagen production, therefore mediating gland EMT and finally inducing fibrosis. However, the interaction between GRK2 and TGF-β1-Smad2/3 pathway remains unknown.

GRK2 interacted with Smad2/3 to positively regulate the activation of TGF-β-Smad signaling

We have described before that hemizygous knockout of GRK2 effectively reduces the fibrosis of glands in SS mice, but what remained to be seen was whether GRK2 deficiency leads to a changed TGF-β1 production. Interestingly, there was no obvious difference in the peripheral blood serum TGF-β1 level between WT SS mice and $GRK2^{+/-}$ SS mice (Fig. 3a), demonstrating that GRK2 mediated SS gland fibrosis may have little relationship with TGF-

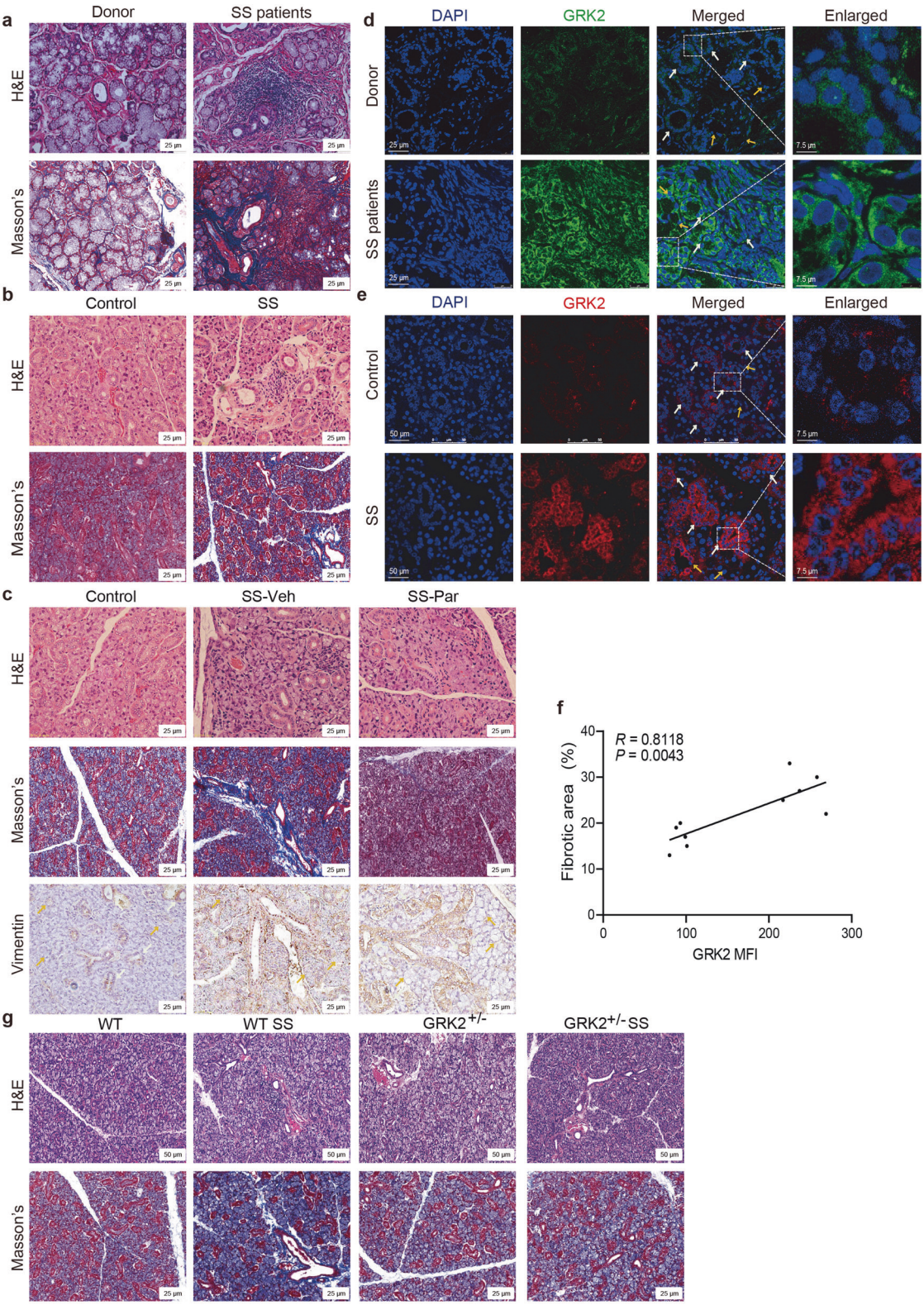

Fig. 1 GRK2 knockdown hindered the gland fibrosis of antigen-induced SS. a H&E staining and Masson's staining of the labial gland tissues in SS patients and healthy donors, Scale bars = 25 μm, $n = 3$. **b** H&E staining and Masson's staining of the SMG tissues in SS and control mice. Scale bars = 25 μm, $n = 5$. **c** Typical microscopic pictures of H&E, Masson's, and immunohistochemical Vimentin-stained mice SMGs. Red arrows indicate lymphocytes, yellow arrows indicate acinar atrophy, and white arrows indicate duct dilation. Scale bars = 25 μm, $n = 5$. **d** Immunofluorescence staining for GRK2 (green) in human labial gland tissues. DAPI (blue) was used to stain nuclei. Yellow arrows indicate acinar atrophy, and white arrows indicate duct dilation. Scale bars = 25 μm (original insets) and 7.5 μm (enlarged insets), $n = 5$. **e** Immunofluorescence staining for GRK2 (red) in mice SMG tissues. DAPI (blue) was used to stain nuclei. Yellow arrows indicate acinar atrophy, and white arrows indicate duct dilation. Scale bars = 50 μm (original insets) and 7.5 μm (enlarged insets), $n = 5$. **f** GRK2 and fibrosis of the correlation analysis. **g** H&E staining (scale bars = 50 μm) and Masson's staining of WT and $GRK2^{+/-}$ mice (scale bars = 25 μm), $n = 5$.

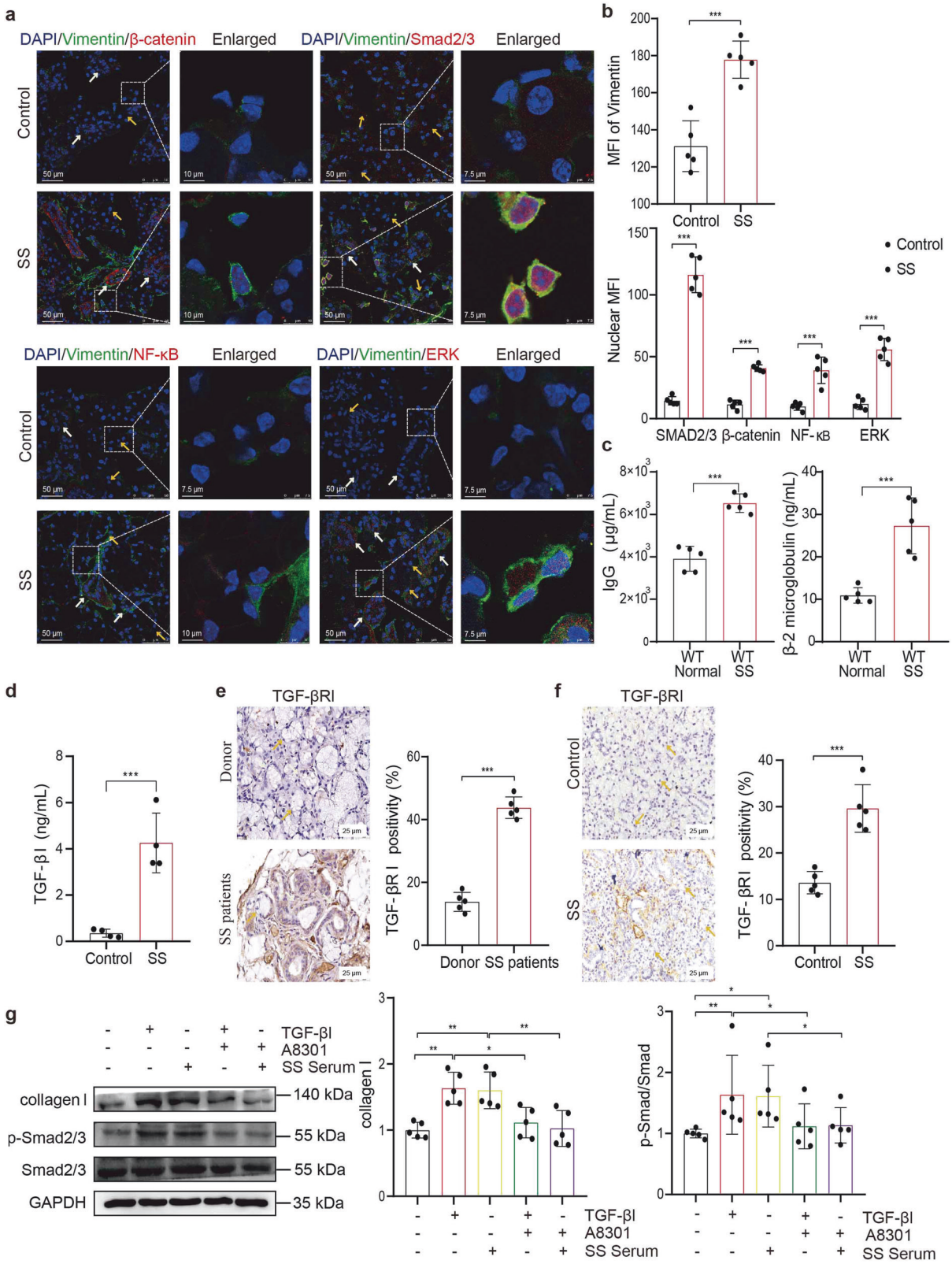

β1 secretion levels. Therefore, it was further investigated whether GRK2 regulates TGF-β1-Smad2/3 signaling. Data indicated that TGF-β1-mediated collagen I expression and Smad2/3 phosphorylation increased in SGECs, which were attenuated by GRK2 inhibitor Par (Fig. 3b). In addition, TGF-β1 treatment increased the ratio of p-Smad2/3 to Smad2/3 and the expression of collagen I in SGECs of WT mice, while TGF-β1 treatment failed to induce Smad2/3 activation and collagen I expression in primary GRK2$^{+/-}$ mouse SGECs (Fig. 3c). Consistent with this, immunofluorescence staining assay confirmed that Smad2/3 was diffusely distributed in

Fig. 2 TGF-β-Smad signaling was markedly activated in SGECs of glands in SS mice. a Immunofluorescence staining for Vimentin (green) and β-catenin, Smad2/3, NF-κB and ERK (red) in mouse SMG tissues. DAPI (blue) was used to stain nuclei. Yellow arrows indicate acinar atrophy, and white arrows indicate duct dilation. Scale bars = 50 μm (original insets) and 7.5–10 μm (enlarged insets). **b** Statistical analysis of Vimentin, β-catenin, Smad2/3, NF-κB and ERK total and nuclear expression. $n = 5$. **c** ELISA was performed to detect the expression of IgG and β2-microglobulin in the serum of SS and control mice, $n = 5$. **d** ELISA was performed to detect the expression of TGF-β1 in the serum of SS and control mice, $n = 5$. **e** Immunohistochemical detection of TGF-βRI expression levels in SS patients. Yellow arrows indicate acinar atrophy, and white arrows indicate duct dilation. Scale bars = 25 μm, $n = 5$. **f** Immunohistochemical detection of TGF-βRI expression levels in SS mice. Yellow arrows indicate acinar atrophy, and white arrows indicate duct dilation. Scale bars = 25 μm, $n = 5$. **g** Mouse SGECs were divided into five groups: control group, TGF-β1 stimulated group, SS serum-stimulated group, A8301 plus TGF-β1 stimulated group and A8301 plus SS serum-stimulated group, and the expression of collagen I, Smad2/3, and p-Smad2/3 was detected by Western blot and analyzed by ImageJ, $n = 5$, values are mean ± standard deviation. $^{*}P < 0.05$, $^{**}P < 0.01$, $^{***}P < 0.001$.

the cytosol of vehicle treated WT mice and GRK2$^{+/-}$ mouse and SGECs, and TGF-β1 stimulation caused the nuclear translocation of Smad2/3 in SGECs of WT SS mice, but not in GRK2$^{+/-}$ SS mice (Fig. 3d). These results suggest that GRK2 promotes the phosphorylation and activation of Smad2/3 and initiates fibrotic morphology of SGECs.

Furthermore, the expressions of GRK2 and Smad2/3 were highly elevated in the labial gland tissues of SS patients, and the colocalization of GRK2 and Smad2/3 was also increased (Fig. 4a–e). Correlation analysis revealed a positive relationship between labial gland GRK2 expression and Smad2/3 nuclear expression in SS patients (Fig. 4f). Importantly, Co-IP assay validated that the co-expression of GRK2 and Smad2/3 increased compared with normal control, while the co-expression decreased after administration with GRK2 inhibitor Par in the SMGs of mice (Fig. 4g). The results suggested that GRK2 interacted with Smad2/3 to positively regulate the Smad2/3 signaling pathway.

Hemizygous knockout of GRK2 prevented Smad2/3 nuclear translocation in vivo and prevented antigen-induced SS

In order to explore the role of GRK2 in regulating TGF-β-Smad2/3 activation and fibrosis process of SS glands in vivo, an antigen-induced SS model in WT and GRK2$^{+/-}$ mice was established, and the cellular localization and expression of Smad2/3 in SMG tissues and global manifestations of SS were compared. Data detailed body weight loss, water consumption, and SMG index were significantly alleviated in GRK2$^{+/-}$ SS mice compared with WT SS mice, along with increased saliva volume (Fig. 5a–d). Ultrasonography revealed that SMG area and blood flow signal was significantly increased in WT SS mice compared with WT control mice, while the GRK2 hemizygous knockout relieved the SMG area and blood flow signal (Fig. 5e–g). Increased secretion of IgG and β-2 microglobulin were observed in the serum of WT SS mice, whereas no significant changes were observed in GRK2$^{+/-}$ SS mice, suggesting that hemizygous knockout of GRK2 significantly mitigated the disease activity in SS mice (Fig. 5h). Importantly, the expression and location of Vimentin and Smad2/3 in SMG tissues from the WT and GRK2$^{+/-}$ mice detected by immunofluorescence staining portrayed that the Vimentin and Smad2/3 expression was greatly increased, and Smad2/3 was mainly distributed in the nucleus in the WT SS mice compared with WT control mice. On the contrary, the expression of Vimentin and Smad2/3 was much lower in the GRK2$^{+/-}$ SS group compared with WT SS mice, and Smad2/3 was constrained to the cytoplasm of SGECs in GRK2$^{+/-}$ SS mice (Fig. 5i). The above results suggest that hemizygous knockout of GRK2 inhibits the activation of Smad2/3 in vivo, prevents gland fibrosis and eventually suppresses antigen-induced SS.

Inhibiting GRK2 significantly attenuated gland fibrosis and alleviated the progression of SS mice

Since the above results demonstrated that GRK2 positively regulated the TGF-β1-Smad2/3 signaling pathway and promoted mouse gland fibrosis, it was next tested if pharmacologically targeting GRK2 with specific inhibitors could ameliorate gland fibrosis and treat antigen-induced SS. After establishing the SS mouse model, the GRK2 inhibitor, Par (5 mg/kg) was individually administered, with another group of SS mice receiving HCQ (80 mg/kg) as a positive control. Twenty-eight days after the first immunization, the salivary flow of SS mice was significantly reduced and the water consumption was elevated compared with the normal group; comparable to Par, or HCQ treatment effectively restored the salivary flow of mice and brought a large reduction in water consumption and SMG index compared with the vehicle treated SS group (Fig. 6a–d).

Ultrasonography results revealed that the area of SMGs in SS mice was significantly increased, and the blood flow signal was also enhanced compared with the normal group; Par, or HCQ administration reduced the area of SMGs and attenuated the blood flow signal in SS mice to different degrees (Fig. 6e–g). A notable elevation of IgG and β-2 microglobulin was observed in WT SS mouse. Following treatment with either Par or HCQ, these levels exhibited a variable reduction, with Par demonstrating a more pronounced decline. This suggests that both Par and HCQ are capable of attenuating the disease activity of SS to a significant extent (Fig. 6h). H&E staining laid bare that compared with normal mice, dilation of ducts, lymphocyte infiltration and pathology score were greatly increased in the SS mice, while these pathological changes in SS mice were successfully improved by drug therapy compared with vehicle treatment, suggesting that Par could effectively ameliorate the manifestation of SS in mice. Moreover, collagen deposition and gland fibrosis observed by Masson's staining were much more severe in the SMGs of SS mice compared with the normal controls. Par, or HCQ administration reduced collagen deposition compared with SS mice. As expected, increased expression of the fibrotic marker Vimentin was found around the blood vessels and ducts of the gland in SMGs of SS mice, and was significantly reduced in all treated mice (Fig. 6i, Supplementary Fig. S3a). The above results indicate that inhibiting GRK2 with Par effectively attenuates gland fibrosis of SS mice and alleviates SS.

The immunofluorescence staining further confirmed that Vimentin expression was elevated in SMG tissues of SS mice which was reduced substantially by Par treatment, while HCQ administration minimally reduced Vimentin expression. Meanwhile, Smad2/3 expression was increased and distributed both in the cytoplasm and nuclei of the SMG tissues in SS mice compared with normal mice, while both expression and nuclear location of Smad2/3 was significantly decreased by administering of Par, while there is no obvious difference between SS mice and HCQ treated ones (Fig. 6j, Supplementary Fig. S3b). These data demonstrate that inhibiting GRK2 with Par exerts a distinct therapeutic effect on reducing gland fibrosis and eventually improves the function of glands in SS mice.

DISCUSSION

SS is a systematic disorder characterized with T and B lymphocytic infiltration in labial glands and SMGs. The evaluation of the action of the disease is typically based on the physical examination,

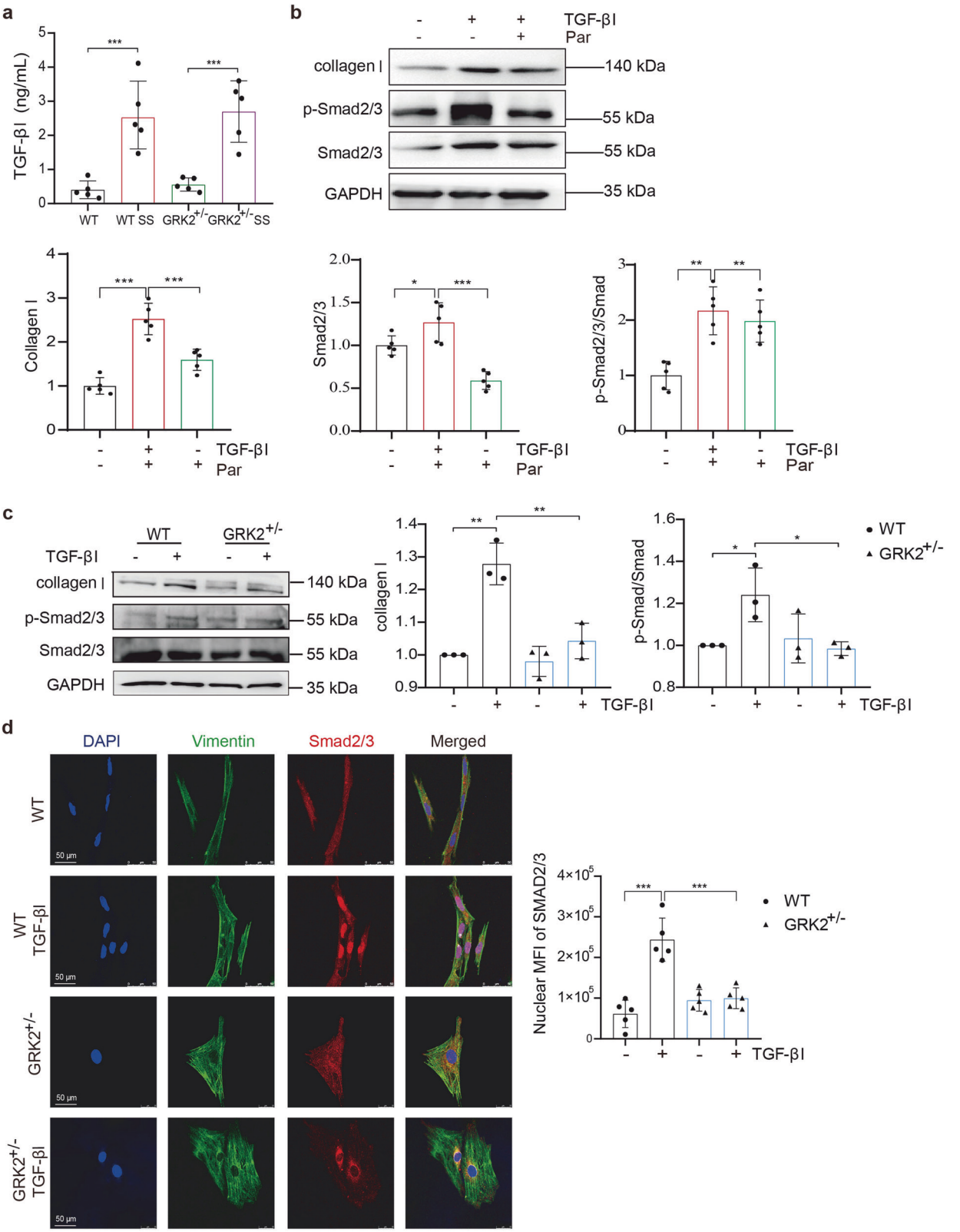

Fig. 3 GRK2 positively regulated the activation of TGF-β-Smad signaling. a The expression levels of TGF-β1 in the peripheral blood serum of WT SS mice and GRK2$^{+/-}$ SS mice were detected by ELISA. $n = 5$. **b** The effect of Par on the expression of collagen I, Smad2/3 and p-Smad2/3 in mouse SGECs stimulated by TGF-β1. $n = 5$. **c** Mouse SGECs from WT and GRK2$^{+/-}$ mice were treated with TGF-β1 or the vehicle control, collagen I, Smad2/3 and p-Smad2/3 expression was detected by Western blot, $n = 3$. **d** Immunofluorescence staining for Vimentin (green) and Smad2/3 (red) on the mouse SGECs treated with TGF-β1 or solvent. DAPI (blue) was used to stain nuclei. And Smad2/3 nucleation expression was analyzed. Scale bars = 50 μm. $n = 5$. *$P < 0.05$, **$P < 0.01$, ***$P < 0.001$.

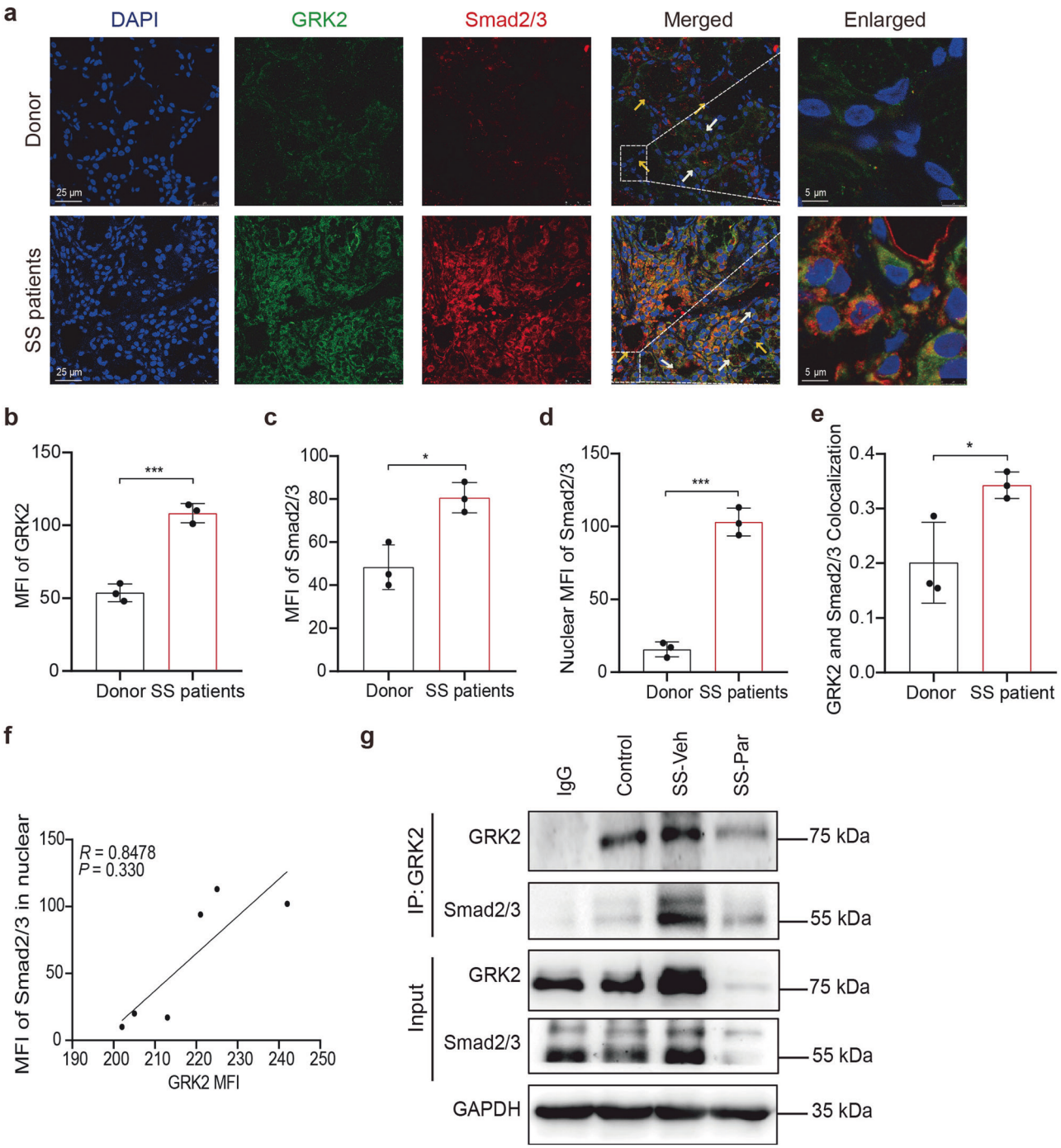

Fig. 4 GRK2 interacted with Smad2/3 in the SMGs of SS mice. a Immunofluorescence staining for GRK2 (green) and Smad2/3 (red) in human labial gland tissues. DAPI (blue) was used to stain nuclei. Yellow arrows indicate acinar atrophy, and white arrows indicate duct dilation. Scale bars = 25 μm (original insets) and 5 μm (enlarged insets), $n = 3$. **b**–**d** The MFI of GRK2 and Smad2/3, and Smad2/3 nuclear expression. **e** The colocalization analysis of GRK2 expression and Smad2/3 nucleus expression in SS patients' labial gland tissues. **f** The correlation analysis of GRK2 and Smad2/3 in SS patients' labial gland tissues. **g** Co-IP experiments were used to verify interaction of Smad2/3 and GRK2 in the WT control, SS-Veh, and SS-Par mice SMGs, $n = 3$. *$P < 0.05$, ***$P < 0.001$.

symptomatology, and the determination of systemic inflammation markers, which are noninvasive. ESSDAI and ESSPRI indices are used for diagnosing SS [34, 35]. Labial gland biopsy can further confirm the diagnosis of SS, but it is invasive and may cause complications including persistent numbness of the biopsy site. In addition, the final diagnosis needs to be combined with clinical symptoms and serological examination with the histology of labial gland biopsy. Currently, the treatment strategies include salivary stimulants, immunosuppression, steroid therapy, and biological therapy [26]. However, the effect of the treatments needs to be improved. Progressive fibrosis of the gland tissue may be the important cause of persistent disruption of glandular function and requires close attention.

TGF-β1-Smad2/3 signaling pathway plays an important role in several types of fibrotic diseases including SS. In patients with SS, gland fibrosis and the activation of TGF-β1-Smad2/3 signaling

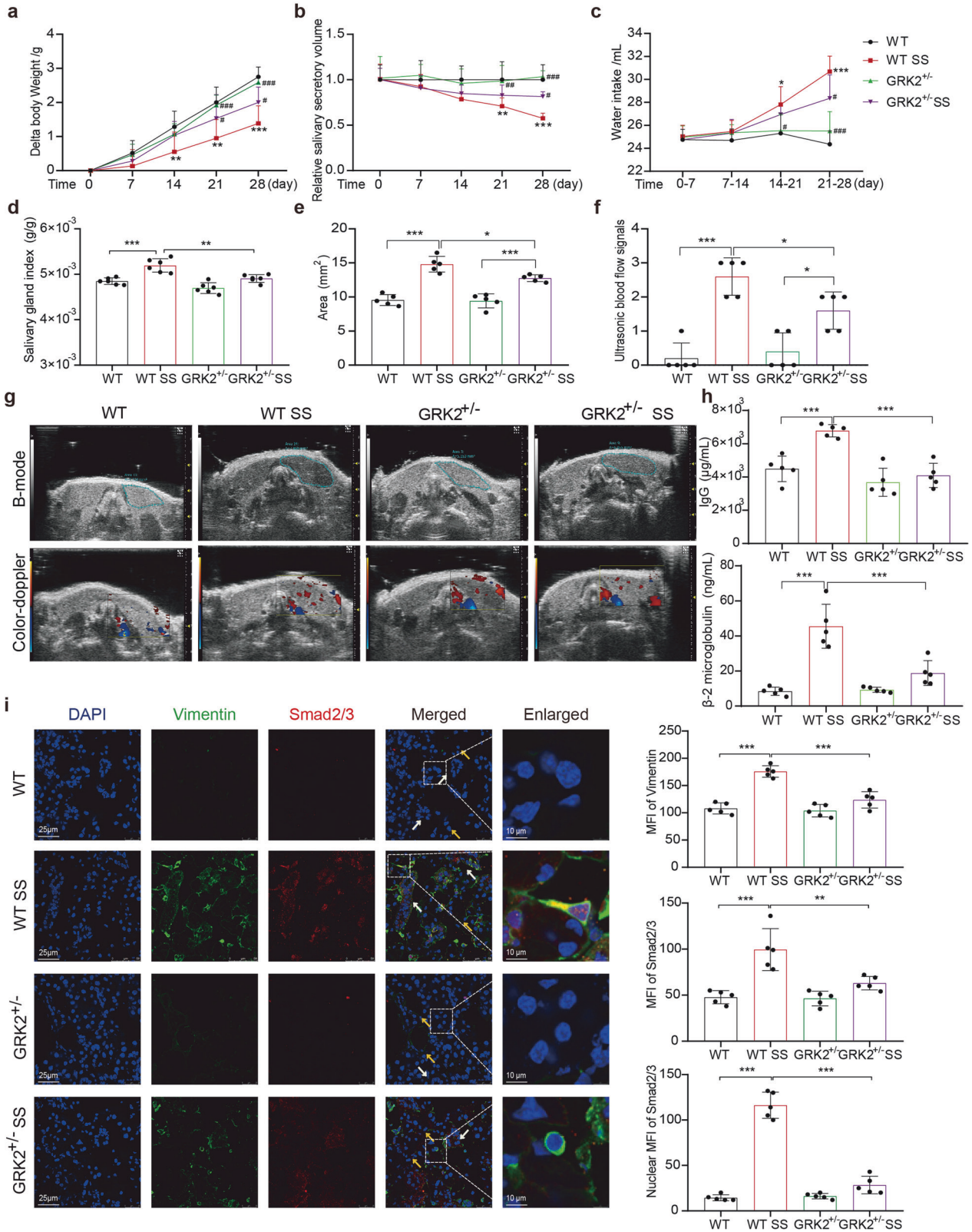

Fig. 5 Hemizygous knockout of GRK2 prevented Smad2/3 nuclear translocation in vivo and effectively improved the manifestations of mice with SS. a–d The SS models of WT and GRK2$^{+/-}$ mice were created, and body weight, salivary volume, water consumption, and SMG index were measured, $n = 5$. **e–g** Score for the mice SMG area and blood flow signal, $n = 5$. **h** ELISA was performed to detect the expression of IgG and β2-microglobulin in the serum of WT and GRK2$^{+/-}$ mice, $n = 5$. **i** Immunofluorescence staining for Vimentin (green) and Smad2/3 (red) on the SMGs of WT SS and GRK2$^{+/-}$ SS mice, and the MFI of Vimentin, Smad2/3, and Smad2/3 nucleation expression. Yellow arrows indicate acinar atrophy, and white arrows indicate duct dilation. Scale bars = 25 μm (original insets) and 10 μm (enlarged insets), $n = 5$. $^{*}P < 0.05$, $^{**}P < 0.01$, $^{***}P < 0.001$. $^{\#}P < 0.05$, $^{\#\#}P < 0.01$, $^{\#\#\#}P < 0.001$ vs SS-Veh.

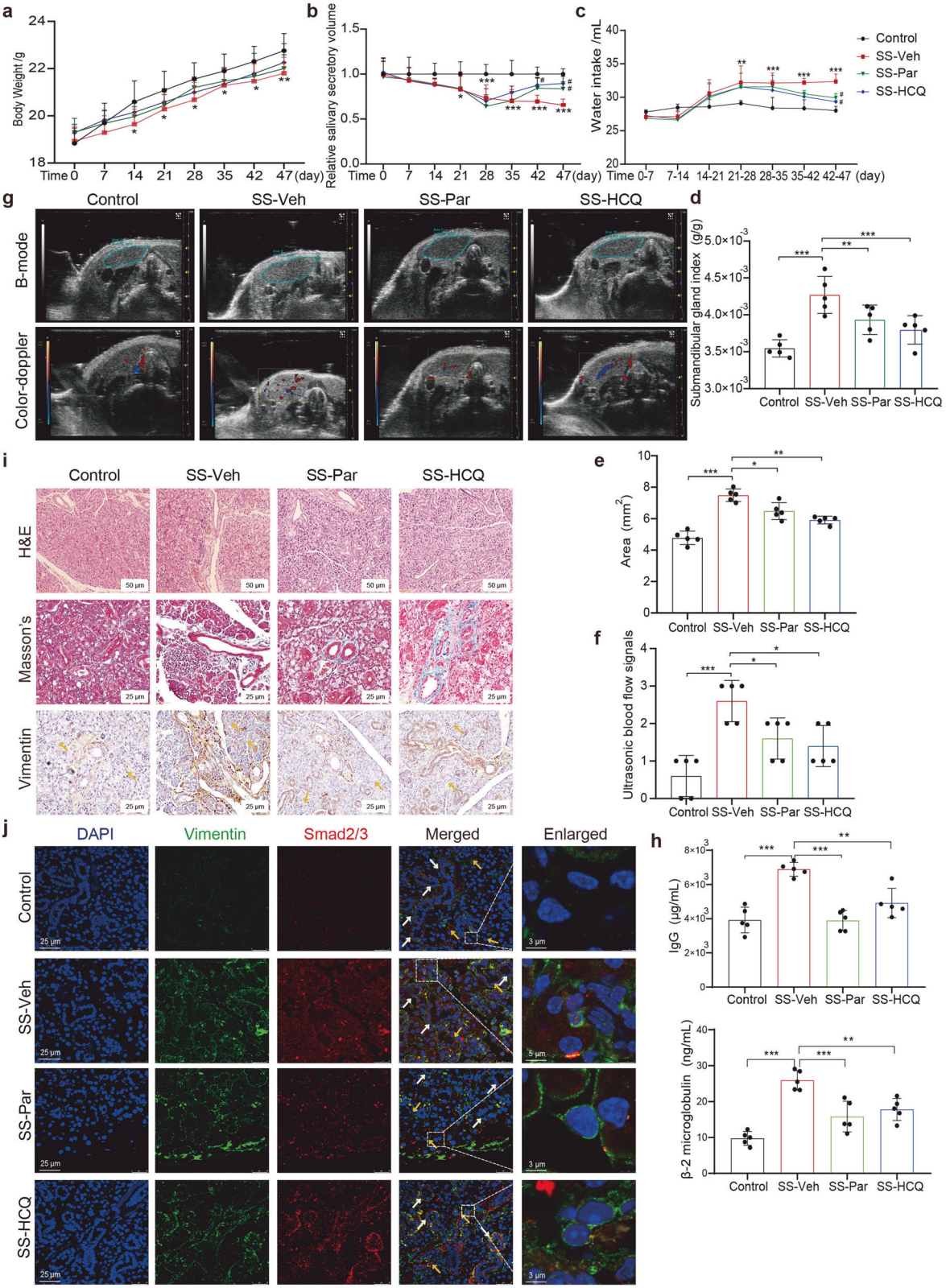

Fig. 6 **Inhibiting GRK2 significantly attenuated gland fibrosis and alleviated the progression of SS mice. a–d** WT SS mice were treated with Par, or HCQ, and body weight, salivary volume, water consumption, and SMG index were measured, $n = 5$. **e–g** Score for the mice SMG area and blood flow signal, $n = 5$. **h** ELISA was performed to detect the expression of IgG and β2-microglobulin in the serum of mice, $n = 5$. **i** H&E (scale bars = 50 μm), Masson's, and Vimentin staining of mice SMGs (scale bars = 25 μm). Yellow arrows indicate acinar atrophy, and white arrows indicate duct dilation. And the analysis results were shown. $n = 5$. **j** Immunofluorescence staining for Vimentin (green) and Smad2/3 (red) in mice SMGs. Yellow arrows indicate acinar atrophy, and green arrows indicate duct dilation. Scale bars = 25 μm (original insets) and 3–5 μm (enlarged insets), $n = 5$. $^{*}P < 0.05$, $^{**}P < 0.01$, $^{***}P < 0.001$ vs control. $^{\#}P < 0.05$ vs SS-Veh.

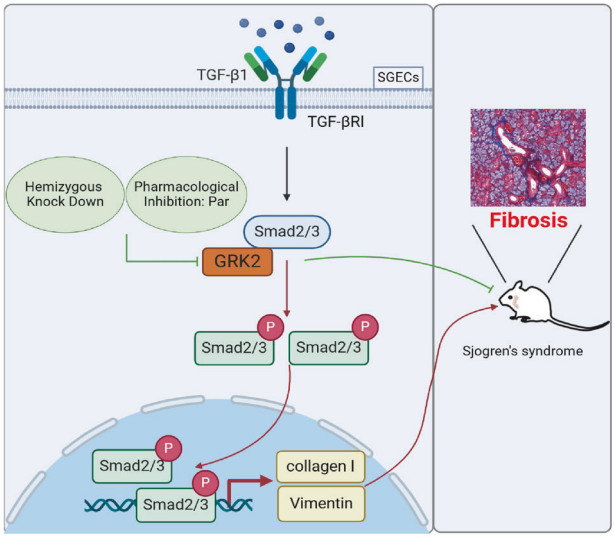

Fig. 7 Schematic summary of the mechanism underlying the actions of GRK2 in antigen-induced SS fibrosis. TGF-β1 binds to its receptor TGF-β1 and activates Smad2/3, which results p-Smad2/3 translocation into the nucleus to upregulate the expression of collagen I and Vimentin, as well as increase the protein expression of GRK2. GRK2 interacts with Smad2/3 to positively regulate the activation of Smad2/3 signaling. Par, as the inhibitor of GRK2, can effectively hinder the formation of the GRK2-Smad2/3 complex, which leads to a reduction in Smad2/3 phosphorylation and nuclear translocation, thus a decreased expression of the target gene of fibrosis.

were observed in the labial glands. When TGF-β1 binds to its receptor, it causes the phosphorylation of Smad2/3, then combines with Smad4 and enters the nucleus to regulate ECM related gene expression, which is termed as the canonical pathway. Several therapeutic candidates targeting TGF-β pathways have been developed or are under development, but the majority have not achieved satisfactory clinical outcomes. For example, TGF-β1 antibody LY2382770 trials for diabetic nephropathy have been ended in phase II because of futility issues [29]. Intracellular targets of canonical Smad for anti-fibrotic therapy have been recognized but have not yet reached clinical trial [11, 27]. The reason for these unsatisfying clinical results may be the uncontrollable non-canonical pathway of TGF-β1 in the progression of fibrosis.

In the present study, it was demonstrated that GRK2 binds to and interacts with Smad2/3 to cooperatively promote SS gland fibrosis in vivo. Consistent with the pathological scores and immunofluorescence staining of the labial gland tissues of SS patients and the SMGs of SS mice, our experimental data depicted that GRK2 was highly expressed in the glandular tissues of SS compared with the glandular tissues of healthy donors or control mice, and the expression of GRK2 was positively correlated with gland fibrosis. Through immunofluorescence staining, immunohistochemical staining and Western blot studies, TGF-β-Smad signaling was found to be markedly activated in SS mouse glands and SGECs of SS mouse glands. Mechanistic studies indicated that inhibition of GRK2 alleviates fibrosis in SS glands by reducing the elevated expression of Vimentin and collagen I via decreasing Smad2/3 phosphorylation/nuclear localization. Smad2/3 was highly expressed in SS glands when compared with healthy ones, and the expression of GRK2 was positively correlated with Smad2/3 activity. Furthermore, GRK2 bound to Smad2/3 in SS mouse glands, and Par significantly reduced this binding. GRK2 is not only induced by TGF-β1 to activate Smad complex, but GRK2 also activates Smad upon co-localization with Smad2/3 in SGECs, indicating the positive feedback loop of TGF-β1-GRK2 contributes to gland fibrosis. Thus, the conclusion here is that GRK2 may be a potential non-canonical TGF-β1 target that plays an important role in the gland fibrosis in SS. Some articles have revealed in tumor cells HepG2 and Huh7 that GRK2 associates with the linker domain of Smad2/3 to prevent nuclear translocation of the Smad complex, thus acting in a negative feedback loop to control TGF-β biological responses [30, 36]. However, many other publications support the viewpoint presented here. Specifically, TGF-β1-mediated collagen I increases from cardiac fibroblasts was attenuated by GRK2 inhibitor Par [22], and GRK2 down-regulates Smad3 expression to attenuate ECM accumulation in lung fibroblast cells [37]. The controversial role of GRK2 plays in TGF-β1-induced signal transduction is probably dependent on the different cell types and different pathological conditions.

In the current work, using SMG antigens to induce a model of SS in WT and GRK2$^{+/-}$ mice, it was found that hemizygous knockout of GRK2 increased saliva secretion, reduced lymphocyte infiltration and collagen deposition in the SMGs of SS mice, and decreased the expression of Vimentin as well as the nuclear translocation of Smad2/3 in the SMGs of SS mice. This indicates GRK2 is involved in the destruction and fibrosis of SMGs in SS mice. In order to further explore the potential therapeutic benefits of targeting GRK2 in SS mice, the mice were treated with Par.

Par has been approved by the USA Food and Drug Administration (FDA) for the treatment of major depressive disorder (MDD), obsessive-compulsive disorder, panic disorder (PD), generalized anxiety disorder, post-traumatic stress disorder (PTSD), and social anxiety disorder (SAD) in adults [38, 39]. It has also been reported that Par exhibits potential therapeutic effect in the treatment of immune diseases such as SLE [40]. However, there is currently no report on whether Par can improve glandular manifestations in SS mice. Our findings demonstrated that Par, acts as a GRK2 inhibitor, significantly enhanced saliva secretion, attenuated lymphocytic infiltration and collagen deposition, and reduced histological scores based on lymphocytic foci. Furthermore, patients with Sjogren's syndrome are prone to depression, and weight loss is a common symptom among depressed individuals [41]. In our study, the body weight of hemizygous knockout of GRK2 or Par treated mice was closer to that of the normal control group than that of the WT-SS group without any significant changes observed. Therefore, we propose that application of Par not only improves glandular fibrosis in SS mice but may also effectively enhance their mental state.

These results indicate that GRK2 may be an important target for the treatment of gland fibrosis in SS. However, Par is associated with increased sedation, constipation, sexual dysfunction, discontinuation syndrome, and weight gain [42, 43]. Nausea is the most commonly reported adverse event related to Par treatment but is generally mild and subsides with continued use [44]. On the other hand, Par treatment has the potential to cause weight gain and sexual dysfunction, primarily anorgasmia and ejaculatory dysfunction for the long term. Thus, it is imperative to further investigate and closely monitor the long-term effects and side effects associated with Par in future studies. In conclusion, we firmly believe that the therapeutic potential of Par outweighs its side effects significantly [44, 45].

HCQ is often recommended as the first treatment for skin or musculoskeletal pain associated with SS [46]. Interestingly, a recent meta-analysis indicated that there is no significant difference between HCQ and placebo for treating either ocular or mouth dryness in SS patients [3, 47]. Our study, which used HCQ as a positive control drug, depicted that the therapeutic effect of HCQ on gland fibrosis in SS mice was not significant.

In this study, GRK2 was demonstrated to positively regulate the phosphorylation of Smad2/3 and activate the TGF-β1-Smad2/3 signaling pathway to promote gland fibrosis. However, GRK2 has many active sites, and different sites will have different effects. The present work only studied how GRK2 interacts with Smad2/3, while the specific

active site of GRK2, and the specific phosphorylation site of Smad2/3 on the GRK2 site needs to be further studied. In addition, although there are many molecular mechanisms of fibrosis, only the TGF-β-Smad2/3 signaling pathway was investigated in this study. Whether there are other molecular mechanisms involved in fibrosis in SS glands is still unclear, and further studies are needed to explore other possible anti-fibrosis therapeutic targets.

In conclusion, our study demonstrated that GRK2 forms a complex with Smad2/3 to interact cooperatively in promoting SS progression. Hemizygous knockout of GRK2 or treatment with GRK2 inhibitor Par, impedes Smad2/3 phosphorylation into nucleus, resulting in disruption of the GRK2-Smad2/3 interaction and suppression of SS gland fibrosis, ultimately improving the fibrosis of glands (Fig. 7). The fibrosis process is almost irreversible; however, the fibrosis is a highly dynamic and progressive process. Antifibrotic treatment may reduce disease progression, slow gland function decline, improve living quality, and affect progression-free survival. Therefore, the interaction between GRK2 and Smad2/3 may be a novel therapeutic target to treat SS or prevent the fibrosis progression of gland.

ACKNOWLEDGEMENTS

This work was financially supported by the National Natural Science Foundation of China (81973314, 82373865, 81973332), the Anhui Provincial Natural Science Foundation for Distinguished Young Scholars (1808085J28), Collaborative Innovation Project of Key Scientific Research Platform in Anhui Universities (GXXT-2020-066), Anhui Provincial Key R&D Programs (2022e07020042), Program for Upgrading Scientific Research Level of Anhui Medical University (2019xkjT008), Academic Funding for Top-notch Talents in University Disciplines (Majors) of Anhui Province (gxbjZD2021047), Anhui Medical University 2022 Provincial New Era Education Quality Project (2022cxcysj081), and Scientific Research Foundation of Anhui Medical University (2023xkj077). We thank Dr. Yi Gao from Department of Pathology, the First Affiliated Hospital of Anhui Medical University for reading the histology images.

AUTHOR CONTRIBUTIONS

RHF and ZWZ performed most of the experiments and wrote the initial manuscript draft. RC, QYG, FH, MLG, and PPG performed experiments, analyzed data, and drew graphs. HXW established the animal models. LLY read the histology images. QTW, WW, and YM designed and directed the study and revised the manuscript. All authors read and approved the final manuscript.

ADDITIONAL INFORMATION

Supplementary information The online version contains supplementary material available at https://doi.org/10.1038/s41401-024-01350-4.

Competing interests: The authors declare no competing interests.

REFERENCES

1. Stefanski AL, Tomiak C, Pleyer U, Dietrich T, Burmester GR, Dörner T. The diagnosis and treatment of Sjögren's syndrome. Dtsch Arztebl Int. 2017;114:354–61.
2. Brito-Zerón P, Baldini C, Bootsma H, Bowman SJ, Jonsson R, Mariette X, et al. Sjögren syndrome. Nat Rev Dis Prim. 2016;2:16047.
3. Negrini S, Emmi G, Greco M, Borro M, Sardanelli F, Murdaca G, et al. Sjögren's syndrome: a systemic autoimmune disease. Clin Exp Med. 2022;22:9–25.
4. Alunno A, Carubbi F, Bistoni O, Caterbi S, Bartoloni E, Mirabelli G, et al. T regulatory and T helper 17 cells in primary Sjögren's syndrome: facts and perspectives. Mediators Inflamm. 2015;2015:243723.
5. Chen X, Zhang P, Liu Q, Zhang Q, Gu F, Xu S, et al. Alleviating effect of paeoniflorin-6′-O-benzene sulfonate in antigen-induced experimental Sjögren's syndrome by modulating B lymphocyte migration via CXCR5-GRK2-ERK/p38 signaling pathway. Int Immunopharmacol. 2020;80:106199.
6. Kiripolsky J, McCabe LG, Kramer JM. Innate immunity in Sjögren's syndrome. Clin Immunol. 2017;182:4–13.
7. Sarrand J, Soyfoo MS. Involvement of epithelial-mesenchymal transition (EMT) in autoimmune diseases. Int J Mol Sci. 2023;24:14481.
8. Sisto M, Tamma R, Ribatti D, Lisi S. IL-6 Contributes to the TGF-β1-mediated epithelial to mesenchymal transition in human salivary gland epithelial cells. Arch Immunol Ther Exp (Warsz). 2020;68:27.
9. Zavadil J, Böttinger EP. TGF-beta and epithelial-to-mesenchymal transitions. Oncogene. 2005;24:5764–74.
10. Sisto M, Lorusso L, Tamma R, Ingravallo G, Ribatti D, Lisi S. Interleukin-17 and -22 synergy linking inflammation and EMT-dependent fibrosis in Sjögren's syndrome. Clin Exp Immunol. 2019;198:261–72.
11. Sisto M, Ribatti D, Lisi S. Sjögren's syndrome-related Organs fibrosis: hypotheses and realities. J Clin Med. 2022;11:3551.
12. Vivino FB, Bunya VY, Massaro-Giordano G, Johr CR, Giattino SL, Schorpion A, et al. Sjogren's syndrome: An update on disease pathogenesis, clinical manifestations and treatment. Clin Immunol. 2019;203:81–121.
13. Yin H, Pranzatelli TJF, French BN, Zhang N, Warner BM, Chiorini JA, NIDCD/NIDCR Genomics and Computational Biology Core. Sclerosing sialadenitis is associated with salivary gland hypofunction and a unique gene expression profile in Sjögren's syndrome. Front Immunol. 2021;12:699722.
14. Chen X, Wu H, Wei W. Advances in the diagnosis and treatment of Sjogren's syndrome. Clin Rheumatol. 2018;37:1743–9.
15. Wang X, Zhang TYZ, Guo ZZ, Pu JC, Riaz F, Feng R, et al. The efficiency of hydroxychloroquine for the treatment of primary Sjögren's Syndrome: a systematic review and meta-analysis. Front Pharmacol. 2021;12:693796.
16. Vivino FB, Carsons SE, Foulks G, Daniels TE, Parke A, Brennan MT, et al. New treatment guidelines for Sjögren's disease. Rheum Dis Clin North Am. 2016;42:531–51.
17. Gottenberg JE, Ravaud P, Puéchal X, Le Guern V, Sibilia J, Goeb V, et al. Effects of hydroxychloroquine on symptomatic improvement in primary Sjögren syndrome: the JOQUER randomized clinical trial. JAMA. 2014;312:249–58.
18. Han CC, Li YF, Zhang YW, Wang Y, Cui DQ, Luo TT, et al. Targeted inhibition of GRK2 kinase domain by CP-25 to reverse fibroblast-like synoviocytes dysfunction and improve collagen-induced arthritis in rats. Acta Pharm Sin B. 2021;11:1835–52.
19. Han CC, Liu Q, Zhang Y, Li YF, Cui DQ, Luo TT, et al. CP-25 inhibits PGE2-induced angiogenesis by down-regulating EP4/AC/cAMP/PKA-mediated GRK2 translocation. Clin Sci (Lond). 2020;134:331–47.
20. Yang XZ, Zhao YJ, Jia XY, Wang C, Wu YJ, Zhang LL, et al. CP-25 combined with MTX/ LEF ameliorates the progression of adjuvant-induced arthritis by the inhibition on GRK2 translocation. Biomed Pharmacother. 2019;110:834–43.
21. Li N, Shan S, Li XQ, Chen TT, Qi M, Zhang SN, et al. G Protein-coupled receptor kinase 2 as novel therapeutic target in fibrotic diseases. Front Immunol. 2022;12:822345.
22. Fu J, Li L, Chen L, Su CP, Feng XL, Huang K, et al. PGE2 protects against heart failure through inhibiting TGF-β1 synthesis in cardiomyocytes and crosstalk between TGF-β1 and GRK2. J Mol Cell Cardiol. 2022;172:63–77.
23. Sisto M, Ribatti D, Lisi S. SMADS-mediate molecular mechanisms in Sjögren's syndrome. Int J Mol Sci. 2021;22:3202.
24. Zhu ZD, Zhang M, Wang Z, Jiang CR, Huang CJ, Cheng HJ, et al. Chronic β-adrenergic stress contributes to cardiomyopathy in rodents with collagen-induced arthritis. Acta Pharmacol Sin. 2023;44:1989–2003.
25. Chisholm DM, Waterhouse JP, Mason DK. Lymphocytic sialadenitis in the major and minor glands: a correlation in postmortem subjects. J Clin Pathol. 1970;23:690–4.
26. Zhan Q, Zhang J, Lin Y, Chen W, Fan X, Zhang D. Pathogenesis and treatment of Sjogren's syndrome: Review and update. Front Immunol. 2023;14:1127417.
27. Zhang X, Yun JS, Han D, Yook JI, Kim HS, Cho ES. TGF-β pathway in salivary gland fibrosis. Int J Mol Sci. 2020;21:9138.
28. Mestre-Torres J, Solans-Laque R. Pulmonary involvement in Sjögren's syndrome. Med Clin (Barc). 2022;158:181–5.
29. Voelker J, Berg PH, Sheetz M, Duffin K, Shen T, Moser B, et al. Anti-TGF-β1 antibody therapy in patients with diabetic nephropathy. J Am Soc Nephrol. 2017;28:953–62.
30. Ho J, Chen H, Lebrun JJ. Novel dominant negative Smad antagonists to TGFbeta signaling. Cell Signal. 2007;19:1565–74.
31. Zhang J, Zhang X, Shi X, Liu Y, Cheng D, Tian Q, et al. CXCL9, 10, 11/CXCR3 axis contributes to the progress of primary Sjogren's syndrome by activating GRK2 to promote T lymphocyte migration. Inflammation. 2023;46:1047–60.
32. Bergum B, Koro C, Delaleu N, Solheim M, Hellvard A, Binder V, et al. Antibodies against carbamylated proteins are present in primary Sjögren's syndrome and are associated with disease severity. Ann Rheum Dis. 2016;75:1494–500.
33. Pertovaara M, Korpela M. Serum β2 microglobulin correlates with the new ESSDAI in patients with Sjögren's syndrome. Ann Rheum Dis. 2011;70:2236–7.
34. Ture HY, Kim NR, Nam EJ. EULAR Sjogren's syndrome patient reported index (ESSPRI) and other patient-reported outcomes in the assessment of glandular dysfunction in primary Sjögren's syndrome. Life (Basel). 2023;13:1991.
35. de Wolff L, Arends S, Pontarini E, Bombardieri M, Bowman SJ, Bootsma H. Development and performance of the Clinical Trials ESSDAI (ClinTrialsESSDAI), consisting of frequently active clinical domains, in two randomised controlled trials in primary Sjögren's syndrome. Clin Exp Rheumatol. 2021;133(Nov-Dec):100–6.

36. Ho J, Cocolakis E, Dumas VM, Posner BI, Laporte SA, Lebrun JJ. The G protein-coupled receptor kinase-2 is a TGFbeta-inducible antagonist of TGFbeta signal transduction. EMBO J. 2005;24:3247–58.
37. Li Y, Sun Y, Wu N, Ma H. GRK2 promotes activation of lung fibroblast cells and contributes to pathogenesis of pulmonary fibrosis through increasing Smad3 expression. Am J Physiol Cell Physiol. 2022;322:C63–C72.
38. Feighner JP, Boyer WF. Paroxetine in the treatment of depression: a comparison with imipramine and placebo. J Clin Psychiatry. 1992;53 Suppl:44–47.
39. Gunasekara NS, Noble S, Benfield P. Paroxetine. An update of its pharmacology and therapeutic use in depression and a review of its use in other disorders. Drugs. 1998;55:85–120.
40. Wang B, Huang Y, Tang Y, Zhao ZX, Shi W, Jian D, et al. Paroxetine is an effective treatment for refractory erythema of rosacea: primary results from the prospective rosacea refractory erythema randomized clinical trial. J Am Acad Dermatol. 2023;88:1300–7.
41. Zhao D, Wu Z, Zhang H, Mellor D, Ding L, Wu H, et al. Somatic symptoms vary in major depressive disorder in China. Compr Psychiatry. 2018;87:32–37.
42. Boyer WF, Feighner JP. An overview of paroxetine. J Clin Psychiatry. 1992;53 Suppl:3–6.
43. Kishi T, Ikuta T, Sakuma K, Okuya M, Hatano M, Matsuda Y, et al. Antidepressants for the treatment of adults with major depressive disorder in the maintenance phase: a systematic review and network meta-analysis. Mol Psychiatry. 2023;28:402–9.
44. Marks DM, Park MH, Ham BJ, Han C, Patkar AA, Masand PS, et al. Paroxetine: safety and tolerability issues. Expert Opin Drug Saf. 2008;7:783–94.
45. Dannon PN, Lowengrub K, Iancu I, Kotler M. Paroxetine in panic disorder: clinical management and long-term follow-up. Expert Rev Neurother. 2004;4:191–8.
46. Ramos-Casals M, Brito-Zerón P, Bombardieri S, Bootsma H, De Vita S, Dörner T, et al. EULAR recommendations for the management of Sjögren's syndrome with topical and systemic therapies. Ann Rheum Dis. 2020;79:3–18.
47. Wang SQ, Zhang LW, Wei P, Hua H. Is hydroxychloroquine effective in treating primary Sjogren's syndrome: a systematic review and meta-analysis. BMC Musculoskelet Disord. 2017;18:186.